(Received 20 September 2025, Accepted 22 October 2025, Scheduled 10 November 2025)

Non-Contact Microwave Sensor for High-Sensitivity Medical Ethanol Concentration Detection Using Coupled Microstrip Coupler

Runlin Zhang[1], Shujiang Zhang[2], and Tao Tang[3,*]

[1] *The 58th Research Institute of China Electronics Technology Group Corporation, Wuxi 214062, China*
[2] *The Affiliated Hospital of Southwest Medical University, Luzhou 646000, China*
[3] *College of Electronics and Information, Southwest Minzu University, Chengdu 610225, China*

ABSTRACT: This paper presents a medical ethanol concentration sensor based on the principles of liquid-coupling loss, which enables rapid and accurate measurement and classification of medical ethanol concentrations. The sensor system consists of integrated circuits for liquid-coupling loss, amplitude detection, signal processing, and visualization. It utilizes variations in RF signal amplitude to determine the concentration. Theoretical analysis, grounded in Bruggeman model, quantitatively correlates the dielectric constant of medical ethanol with its concentration, thereby establishing a robust theoretical foundation for the sensor design. Experimental validation demonstrates the sensor's ability to precisely differentiate among medical ethanol concentrations of 95%, 75%, and 50% at test frequencies of 1 GHz, 2 GHz, and 3 GHz. The agreement between empirical data and theoretical predictions confirms the sensor's efficacy and reliability. Key advantages include user-friendly operation, cost efficiency, and intuitively presented results, rendering the sensor highly suitable for broad medical applications.

1. INTRODUCTION

Ethanol is a widely used medical supply that plays a pivotal role in healthcare facilities across the globe. As medical technology advances, varying concentrations of medical ethanol have distinct applications in clinical settings. For instance, 25% to 50% ethanol solutions are commonly employed for physical cooling, allowing feverish patients to benefit from a cooling effect through ethanol wipes. Meanwhile, 75% ethanol, recognized for its potent disinfection properties, is extensively utilized for wound treatment to mitigate infection risks. Additionally, 95% ethanol is frequently used for cleaning ultraviolet lamps and other medical equipment within hospitals [1]. However, ethanol's volatility introduces challenges in its storage and management. Improper storage conditions can lead to concentration reductions due to evaporation, while inadequate management or unclear labeling can result in confusion among different ethanol types. These issues may lead to medical staff inadvertently using or mishandling the incorrect type of ethanol, posing a significant threat to patient safety [2]. Consequently, the regular maintenance and inspection of liquid medical supplies, such as medical ethanol, are imperative.

Current methods for detecting medical ethanol concentration can be broadly classified into laboratory-based analytical techniques and portable sensor approaches, each with specific limitations that hinder clinical adoption:

1) Laboratory-based methods:

Gas chromatography (GC): While achieving $< 1\%$ measurement error [3, 4], this method requires expensive instrumentation (systems costing $> 10\,\text{k}$) [5], complex operational protocols, and time-consuming analysis, making it unsuitable for real-time detection.

Infrared spectroscopy: Provides non-contact, high-precision measurements by analyzing ethanol's infrared absorption characteristics. However, its implementation is constrained by high equipment costs and the need for specialized operator expertise [5].

Refractive index measurement: Determines concentration through refractive index variations, offering simplicity and rapid response. Nevertheless, its accuracy is highly susceptible to temperature fluctuations and ambient light interference, particularly ineffective for high-concentration ethanol.

Density measurement: Relies on the density-concentration relationship for higher precision but necessitates precision balances and intricate procedures, limiting rapid deployment in clinical environments.

Conductivity measurement: Leverages solution conductivity correlations with concentration. Despite simple equipment requirements, measurement stability is compromised by ionic impurities in solutions [6].

Optical rotation: Measures ethanol solution optical rotation with high precision but is restricted to specific ethanol types, severely limiting general applicability.

2) Portable sensor approaches:

* Corresponding author: Tao Tang (tangt@swun.edu.cn).

Electrochemical sensors: Enable real-time monitoring through redox reactions but suffer from electrode drift, exhibiting 15% accuracy degradation after 100 measurement cycles [7, 8].

Optical sensors: Utilize light interaction principles for rapid detection but demonstrate significant performance variations (>30% signal drift) under ambient light fluctuations [9–11].

While these methods provide diverse options for ethanol concentration detection, they collectively face critical challenges: laboratory techniques (GC, infrared spectroscopy, etc.) are hindered by high costs and operational complexity, whereas portable sensors (electrochemical/optical types) struggle with long-term stability and environmental robustness. Thus, developing a medical ethanol concentration detection method that is user-friendly, cost-effective, and provides highly visualized results is of practical importance.

This paper presents a non-contact microwave sensor that addresses these challenges through the following key innovations: First, it simplifies the detection process, eliminating the need for complex procedures, and making it accessible to general medical personnel. Second, it provides real-time visualization of detection results, offering an intuitive and easy-to-understand output that facilitates rapid assessment of whether the ethanol concentration meets standards and if the ethanol type is correctly identified. Third, it is cost-effective and reusable, making it suitable for mass production and broad application. Additionally, the sensor demonstrates strong resistance to environmental interference, ensuring stable performance in complex medical environments. The sensor operates on the liquid-coupling loss principle, determining ethanol concentration by assessing the attenuation characteristics of specific-frequency signals in ethanol solutions. Compared to existing methods, this non-contact approach offers significant advantages in terms of simplicity, intuitiveness, cost-effectiveness, and robustness.

2. DESIGN SCHEME FOR SENSOR SYSTEM

The sensor system introduced in this paper is designed to measure the compliance of medical ethanol concentration and differentiate among various concentrations. During operation, when an ethanol sample is introduced into the designated sensing region of the sensor, the resultant variation in the amplitude of the microwave signal is directly translated into a visual output, indicated by the number of illuminated LEDs in an array. This streamlined process, which requires no additional operator intervention, qualifies the design as a non-contact microwave sensor. Comprising a liquid-coupling loss circuit, a detection circuit, a signal processing circuit, and a visualization circuit (as depicted in Fig. 1), the system operates on the principle of the correlation between the dielectric constant of medical ethanol and its concentration. When being applied to the radio frequency (RF) microstrip coupler, different concentrations of medical ethanol cause varying degrees of change in the RF signal amplitude. Measuring these changes allows the sensor to assess concentration compliance and differentiate among various levels.

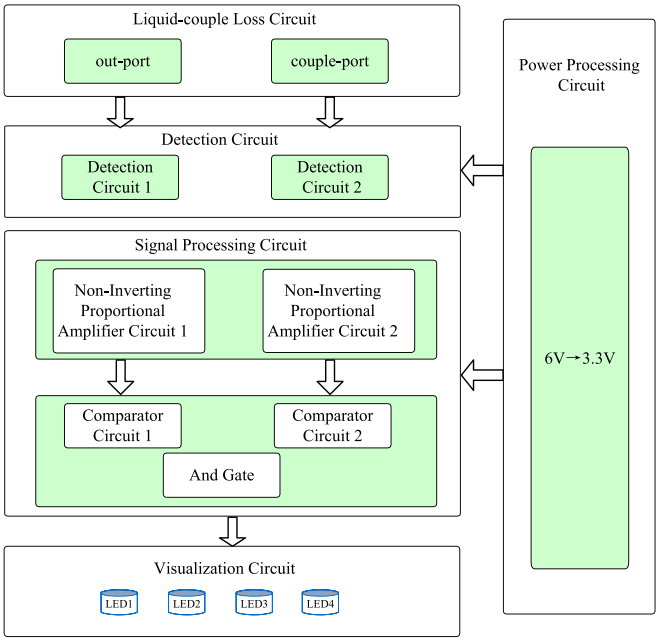

FIGURE 1. Sensor circuit system diagram.

2.1. Liquid-Coupling Loss Circuit

Liquid-coupling loss circuit is central to the sensor, transforming differences in medical ethanol's dielectric constant into variations in the coupling port's output signal amplitude. The ethanol's dielectric constant, when being applied to the RF microstrip coupler, modifies the RF signal's propagation characteristics, leading to changes in the coupling port's output amplitude. This change is directly linked to the ethanol's concentration, establishing a foundation for subsequent detection and processing.

2.2. Detection Circuit

The detection circuit converts the coupling port's output signal amplitude changes into voltage variations. Utilizing a detection circuit enables the conversion of RF signal amplitude changes into DC voltage changes, facilitating quantifiable measurement of these changes. This voltage output becomes the input signal for the subsequent signal processing stage.

2.3. Signal Processing Circuit

Signal processing circuit amplifies and compares the voltage signals from the detection circuit. A proportional amplifier first enhances voltage differences to boost measurement sensitivity and accuracy. Multiple comparators then contrast these amplified signals with a set of gradient reference voltages, producing high- or low-level signals that indicate compliance and concentration differentiation.

To achieve simultaneous compliance measurement and differentiation, the sensor system includes detection and signal processing circuits for both the through and coupling ports of the liquid-coupling loss circuit. For through-port detection, the comparator's reference voltage is set based on detected voltages from tested medical ethanol samples of varying concentrations.

A high-level signal is output if the tested ethanol meets the concentration standard; otherwise, a low-level signal is emitted.

For coupling-port detection, gradient reference voltages are established by analyzing the impact of different ethanol concentrations on coupling degree, with signal processing mirroring that of the through port. The outputs of both detection and processing circuits connect to an AND gate circuit, driving the visualization circuit. This visualization circuit, featuring multiple positioned LEDs, intuitively displays whether the medical ethanol's concentration meets standards and specifies the concentration range through selective LED illumination.

2.4. Visualization Circuit

The visualization circuit, composed of multiple positioned LEDs, displays measurement results based on signals from the signal processing circuit. Specific LED illumination clearly indicates whether the medical ethanol's concentration is compliant and within a particular range, enhancing measurement intuitiveness and readability for medical personnel.

The integrated operation of these circuits enables rapid, accurate measurement of medical ethanol concentration with intuitive feedback. Designed for simplicity, cost-effectiveness, ease of operation, and strong environmental interference resistance, the sensor is well-suited for medical applications.

3. THEORETICAL RELATIONSHIPS BETWEEN ETHANOL CONCENTRATION AND DIELECTRIC CONSTANT

Medical ethanol, a mixture of ethanol and water, has its relative permittivity calculated through various methods, with common approaches including fractional calculation method and Bruggeman model method [12–15]. Bruggeman model is particularly noted for providing more accurate results when addressing interactions between different substances.

This model introduces a generalized Maxwell-Garnett coefficient to account for the effects of the number density and shape of each phase. It thereby establishes a relationship between concentration-dependent permittivity and the material's composition and structure. For medical ethanol, a binary mixture, the relative permittivity can be calculated using Eq. (1) from the Bruggeman model:

$$\frac{f_1}{\varepsilon_1 - \varepsilon_{\min}} + \frac{f_2}{\varepsilon_2 - \varepsilon_{\min}} = 0 \tag{1}$$

Here, $\varepsilon_{\min}$ denotes the effective permittivity of the mixture, and f_1 and f_2 denote the volume fractions of the two liquid components, while ε_1 and ε_2 represent their respective relative permittivities. The varying proportions of ethanol and water in medical ethanol of different concentrations lead to differences in its permittivity. Utilizing Eq. (1), the permittivity values for medical ethanol at various concentrations can be computed, with the results presented in Table 1.

TABLE 1. Dielectric constant of ethanol at different concentrations.

No.	Ethanol Concentration	Dielectric Constant
1	50%	52.5
2	75%	38.75
3	95%	27.75

4. THE CIRCUIT DESIGN

4.1. Liquid-Couple Loss Circuit

The design of the liquid-coupling loss circuit within the sensor circuit system is depicted in Fig. 2. This circuit utilizes a broadband coupler capable of transmitting signals across a 1 GHz to 5 GHz frequency range. Regions ABCD are designated for ethanol drop detection. RF signal is introduced via the input port, with the first detection and signal processing circuit linked to the coupler's output port, while the second circuit monitors the coupling port's output amplitude. Both signal pathways track variations in signal amplitude.

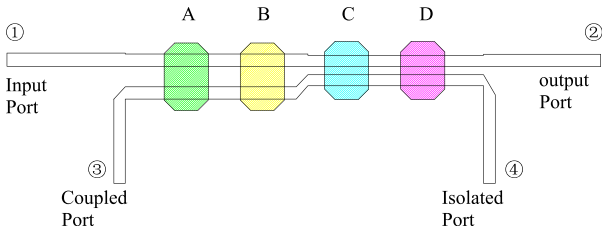

FIGURE 2. Liquid-coupling loss circuit mode.

Simulations using 3D software confirm that introducing ethanol to any of the ABCD regions induces comparable amplitude responses at both the coupled and through ports. Specifically, in region B, simulations conducted with 3D software reveal that introducing ethanol of varying concentrations into the shaded area alters the coupling port's output amplitude, as illustrated in Fig. 3.

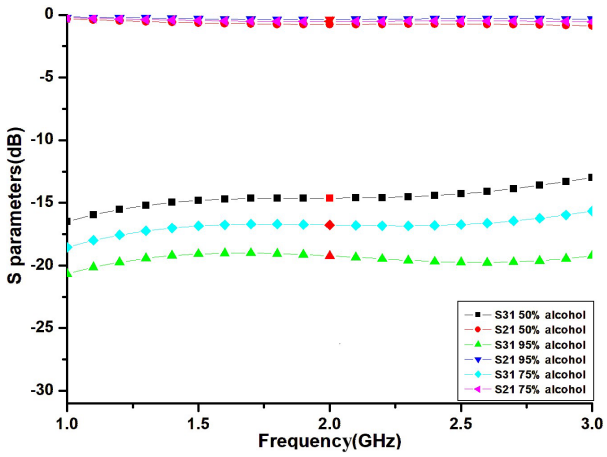

FIGURE 3. S-parameter simulation data for different ethanol concentrations dropped into area B.

4.2. Detection Circuit

Similar to the diode detection method [16], this design employs a logarithmic detection circuit centered around the HMC1094 chip [17]. This circuit transforms differences in the dielectric constants of ethanol at various concentrations into corresponding variations in the detection circuit's output signal amplitudes,

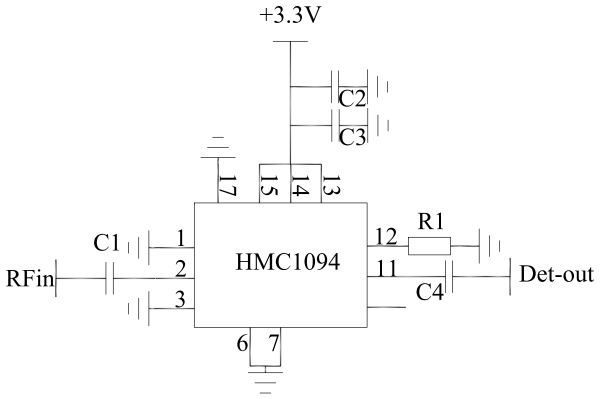

FIGURE 4. Detection circuit.

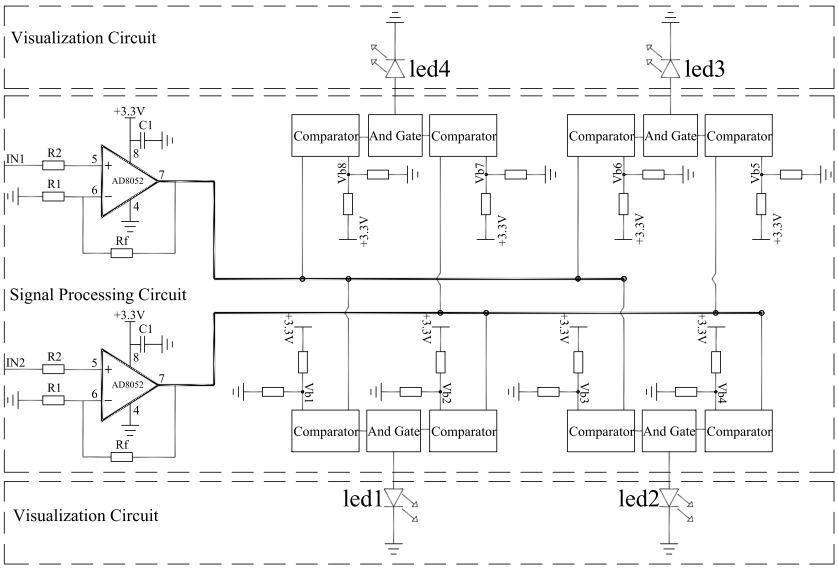

FIGURE 5. Signal processing circuit and visualization circuit design.

which are subsequently converted into voltage differences by the logarithmic detection circuit. Amplitude detection circuits, with HMC1094 chip as the core component, are implemented at both the through and coupling ports of the RF microstrip coupler, with both logarithmic detection circuits being identical. The principle of a single detection circuit is depicted in Fig. 4.

4.3. Signal Processing and Visualization Circuit

Signal processing circuit consists of a set of proportional amplifier circuits and a set of comparator circuits, as illustrated in Fig. 5. The proportional amplifier amplifies output voltage values from the detection circuit, which have varying amplitudes, thereby enhancing the voltage differences. The amplified voltage then serves as the input to the comparator circuit. When both the output port and coupled port comparator circuits output high-level signals, these signals are fed into an AND gate circuit, which subsequently outputs a high-level signal. This high-level output illuminates the corresponding LED. Four LED channels are implemented, with distinct positions and quantities of illuminated LEDs indicating varying signal losses through the detection circuit, thereby reflecting different ethanol concentrations (Table 2).

TABLE 2. Relationship between LED illumination and signal level.

Illuminated LEDs	Input Frequency	Ethanol Concentration
LED1	1 (GHz) (Primary)	50%
LED1-LED2	2 (GHz) and 3 (GHz)	75%
LED1-LED3	(Re-test)	95%
LED1-LED4	/	Others

The signal visualization design prioritizes low power consumption and high reliability, eschewing traditional MCU-driven screen displays. Instead, it employs an LED array where varying positions and quantities of illuminated LEDs represent signal differences through the detection circuit. Each LED consumes only 0.06 W, simplifying the circuit design while ensuring low failure rates and high reliability.

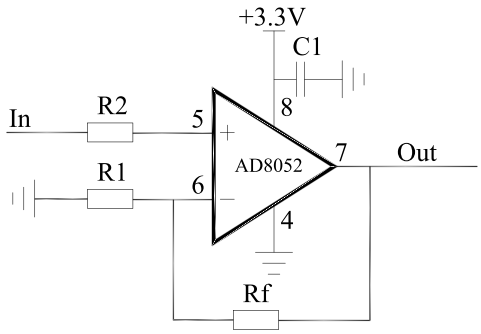

FIGURE 6. Non-inverting proportional amplifier circuit.

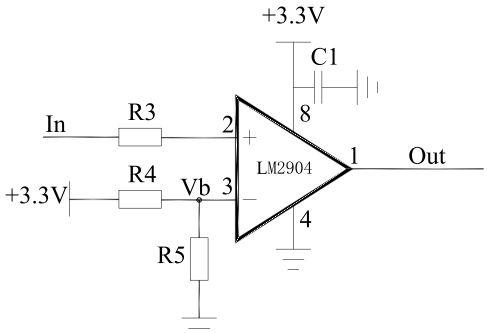

FIGURE 7. Comparator circuit.

TABLE 3. Test results.

Ethanol Category	Test Signal (GHz/dBm)	Coupled Port Reference Voltage (V)	Output Port Reference Voltage (V)	Simulated Coupling (dB)	Measured Coupling (dB)	LED Number	LED Results
95%	1.0/+2	2.419	3.1	21.63	23.83	1–3	correct
	2.0/+2	2.386	3.1	19.57	21.77	1–3	correct
	3.0/+2	2.37	3.097	18.93	21.03	1–3	correct
75%	1.0/+2	2.5	3.068	18.80	19.58	1–2	correct
	2.0/+2	2.486	3.067	17.30	18.76	1–2	correct
	3.0/+2	2.466	3.065	15.81	16.93	1–2	correct
50%	1.0/+2	2.602	3.036	16.71	17.95	1	correct
	2.0/+2	2.583	3.035	14.72	15.98	1	correct
	3.0/+2	2.567	3.032	12.35	13.59	1	correct

In the design, judgment accuracy is increased by continuously optimizing the difference setting between the input detection voltage and reference voltage of the subsequent comparison and drive circuit. There are already numerous design cases and parameter setting methods for in-phase proportional amplification circuits and comparator circuits [18–20], so they will not be elaborated here. The principles and chip models used are shown in Fig. 6 and Fig. 7.

$$A_u = 1 + \frac{R_f}{R_1} \tag{2}$$

Figure 6 depicts the non-inverting operational amplifier, whose gain is given by Eq. (2), where A_u is the overall gain, and $1 + R_f/R_1$ is the in-phase proportional gain. Fig. 7 illustrates the voltage comparator, in which V_b denotes the reference-voltage set-point that can be adjusted by varying the resistor ratio $R_4 : R_5$, thereby altering the comparator reference voltage [21, 22].

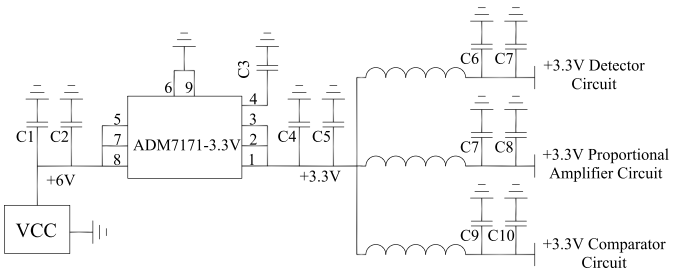

FIGURE 8. Power processing circuit.

4.4. Power Processing Circuit

The digital power supply output voltage is regulated via a low-noise linear voltage regulator chip, as Fig. 8 shows, ADM7171, to achieve secondary voltage regulation. The regulated +3.3 V is isolated using a ferrite bead to power the detector, proportional amplifier circuit, and comparator circuit. Capacitive filtering is implemented at the power supply input terminals of each digital circuit.

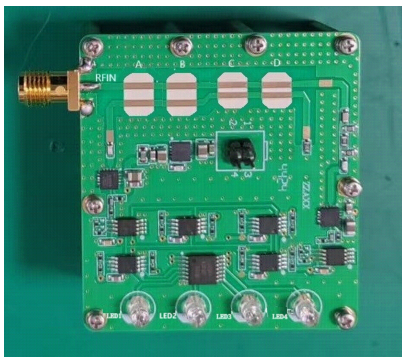

FIGURE 9. Sensor prototype.

TABLE 4. Comparison with previous related works.

Ref.	Sensing Mechanism	Reusability	Visual Readable	Limitations
[23]	Microfluidic channel coupled to a band-pass filter	YES	NO	Consumables, bench-top equipment
[24]	Step-impedance resonator (SIR)	NO	NO	Requires VNA; mechanical fragility; no instant decision
[25]	CSRR-loaded microstrip	NO	NO	Complex fabrication; oxidation reduces repeatability; PC needed
Here	Liquid coupling; logarithmic detection; LED array	YES	YES	Classifies only three medical levels (50%, 75%, 95%); no continuous readout

5. EXPERIMENTAL RESULTS AND ANALYSIS

The fabricated prototype is shown in Fig. 9. For testing, a Rohde & Schwarz (R&S) SMA100B signal generator was used, which has an output frequency range of 8 kHz to 31.8 GHz, sufficient to cover the required test frequencies (1 GHz to 3 GHz). Test frequencies of 1 GHz, 2 GHz, and 3 GHz were selected, with the signal power set to $+2$ dBm. Voltage measurements were performed using a high-precision multimeter. The sensor's response characteristics were recorded by adjusting the output frequency and power of the signal generator.

The results align with theoretical predictions, confirming the sensor's ability to accurately distinguish different concentrations of medical ethanol. The measurement results are intuitively displayed via the on/off status of the LED lights, meeting the design requirements. Typical input and output results of the sensor are summarized in Table 3. Table 4 shows comparison of the proposed work with previous related works, from which it can be seen that our new design has certain advantages.

6. CONCLUSIONS

This paper presents a medical ethanol concentration detection sensor based on the liquid-coupling loss principle, which aims to enable rapid and accurate measurement and classification of medical ethanol concentration. Through theoretical analysis, a quantitative relationship between the concentration of medical ethanol and its dielectric constant was established using the Bruggeman model. This relationship, which arises from the different dielectric properties of ethanol and water, provides the theoretical foundation for detecting concentration changes via amplitude variations in RF signals. A sensor system integrating a liquid-coupling loss circuit, detection circuit, signal processing circuit, and visualization circuit was developed. The liquid-coupling loss circuit converts differences in the dielectric constant of ethanol into RF signal amplitude changes, which are then measured and amplified by high-precision logarithmic detection and signal processing circuits. The ethanol concentration is intuitively displayed using lit and unlit LED lights. Experimental results demonstrate that the sensor can accurately distinguish concentrations of 95%, 75%, and 50% medical ethanol at test frequencies of 1 GHz, 2 GHz, and 3 GHz, confirming the effectiveness and reliability of the sensor design.

ACKNOWLEDGEMENT

Shujiang Zhang and Runlin Zhang made equal contributions to this article. This work was supported by the Southwest Minzu University Research Startup Funds (No. RQD2024009), and the Sichuan Provincial Science and Technology Department Key Project (No. 2025YFHZ0013).

REFERENCES

[1] Le Daré, B. and T. Gicquel, "Therapeutic applications of ethanol: A review," *Journal of Pharmacy and Pharmaceutical Sciences*, Vol. 22, No. 1, 525–535, 2019.

[2] Halsall, L., P. Irizar, S. Burton, S. Waring, S. Giles, L. Goodwin, and A. Jones, "Hazardous, harmful, and dependent alcohol use in healthcare professionals: A systematic review and meta-analysis," *Frontiers in Public Health*, Vol. 11, 1304468, 2023.

[3] Miricioiu, M. G., V. Niculescu, O. R. Dinca, F. Mitu, and M. E. Craciun, "Analytical errors in routine gas chromatography analysis," *Revista de Chimie*, Vol. 67, No. 3, 396–400, 2016.

[4] Drolc, A., P. Djinović, and A. Pintar, "Gas chromatography analysis: Method validation and measurement uncertainty evaluation for volume fraction measurements of gases in simulated reformate gas stream," *Accreditation and Quality Assurance*, Vol. 18, No. 3, 225–233, 2013.

[5] Monad Lab Tech, "How much is a gas chromatography machine? Understanding costs and considerations," https://monadlabtech.com/blogs/how-much-is-a-gas-chromatography-machine-understanding-costs-and-considerations, 2024.

[6] Cengiz, C., M. Konstantinou, M. Harkes, D. Boonstra, A. R. Piedrabuena, and A. Talmon, "Application of concentration conductivity measurement (CCM) for porosity and density profiling in granular media," *Measurement*, Vol. 245, 116644, 2025.

[7] Biscay, J., E. Findlay, and L. Dennany, "Electrochemical monitoring of alcohol in sweat," *Talanta*, Vol. 224, 121815, 2021.

[8] Shaver, A. and N. Arroyo-Currás, "The challenge of long-term stability for nucleic acid-based electrochemical sensors," *Current Opinion in Electrochemistry*, Vol. 32, 100902, 2022.

[9] Parthasarathy, S., V. Nandhini, D. Prakalya, and B. G. Jeyaprakash, "Light-assisted ethanol sensor at ambient temperature using spray deposited ZnO thin films," *International Journal of ChemTech Research*, Vol. 7, No. 2, 974–4290, 2015.

[10] Mourya, V., S. Yadav, P. Lohia, A. C. Mishra, D. K. Dwivedi, and U. Kulshrestha, "High-precision alcohol sensing using twin core photonic crystal fiber," *Photonics and Nanostructures — Fundamentals and Applications*, Vol. 63, 101348, 2025.

[11] Jiang, Y., Y. Yi, G. Brambilla, and P. Wang, "High-sensitivity, fast-response ethanol gas optical sensor based on a dual microfiber coupler structure with the Vernier effect," *Optics Letters*, Vol. 46, No. 7, 1558–1561, 2021.

[12] Escalante-Martinez, J. E., L. J. Morales-Mendoza, C. Calderon-Ramon, L. D. R. Juarez, E. S. Paredes, J. V. Garcia, J. R. Laguna-Camacho, S. N. Gonzalez-Rocha, E. Mejia-Sanchez, J. Garrido-Melendez, H. Lopez-Calderon, and J. Martinez-Castillo, "Fractional derivatives modeling dielectric properties of biological tissue," in *2018 IEEE XXV International Conference on Electronics, Electrical Engineering and Computing (INTERCON)*, 1–3, Lima, Peru, 2018.

[13] Tuncer, E. and G. A. Niklasson, "Properties of Bruggeman dielectric mixture expression," in *2014 IEEE Conference on Electrical Insulation and Dielectric Phenomena (CEIDP)*, 875–878, Des Moines, IA, USA, 2014.

[14] Rotaru, C., C. Flueraru, S. Nastase, and I. Rotaru, "Dielectric function evolution as Bruggeman method solution," in *1997 International Semiconductor Conference 20th Edition, CAS'97 Proceedings*, Vol. 2, 447–450, Sinaia, Romania, 1997.

[15] Goyal, N. and R. Panwar, "Dielectric characterization of electromagnetic mixing model assisted optimization derived heterogeneous composites for stealth technology," *IEEE Transactions on Dielectrics and Electrical Insulation*, Vol. 30, No. 2, 690–699, 2023.

[16] Ivanov, S. I. and A. P. Lavrov, "Optimal operation modes of low cost RF power diode detector on multi-tone signals," in *2018 International Symposium on Consumer Technologies (ISCT)*, 51–53, St. Petersburg, Russia, 2018.

[17] Hao, X., Y. Zheng, F. Tian, Q. Zhou, H. Li, Z. Liu, J. Liu, and H. Liao, "A reverse-RSSI logarithmic power detector with +35-dBm maximum detectable power in 180-nm CMOS," *IEEE Microwave and Wireless Components Letters*, Vol. 29, No. 9, 610–613, 2019.

[18] Yoo, M., S. Kang, B. Jin, H. Son, K. Kim, J. Wi, G. Nam, N. H. Bae, and H. Ko, "Low-noise operational amplifier using dual-path dual-chopper fill-in technique," *IEEE Sensors Journal*, Vol. 24, No. 8, 12 550–12 559, 2024.

[19] Aiello, O., P. Crovetti, P. Toledo, and M. Alioto, "Rail-to-rail dynamic voltage comparator scalable down to pW-range power and 0.15-V supply," *IEEE Transactions on Circuits and Systems II: Express Briefs*, Vol. 68, No. 7, 2675–2679, 2021.

[20] Ishii, T., S. Ning, M. Tanaka, K. Tsurumi, and K. Takeuchi, "Adaptive comparator bias-current control of 0.6 V input boost converter for ReRAM program voltages in low power embedded applications," *IEEE Journal of Solid-State Circuits*, Vol. 51, No. 10, 2389–2397, 2016.

[21] Summatta, C., T. Phurahong, W. Rattanangam, and W. Chaiyong, "Low-cost and compact window comparator circuit with MOSFET-resistor voltage references," in *2019 IEEE 2nd International Conference on Power and Energy Applications (ICPEA)*, 75–78, Singapore, 2019.

[22] Summatta, C. and T. Phurahong, "Three-stage window comparator circuit with MOSFET-resistor voltage reference," in *2020 3rd International Conference on Power and Energy Applications (ICPEA)*, 37–40, Busan, Korea (South), 2020.

[23] Nguyen, T.-K. and C.-H. Tseng, "New radio-frequency liquid permittivity measurement system using filter-based microfluidic sensor," *IEEE Sensors Journal*, Vol. 23, No. 12, 12 785–12 795, 2023.

[24] Liu, W. and L. Xu, "Dual-band microwave sensor for sensing application of microfluidic based on transmission line loaded pair of SIR resonators," *IEEE Transactions on Instrumentation and Measurement*, Vol. 73, 1–11, 2024.

[25] Song, Y., E. Wu, P. Zhao, C. Wang, M. Parkhomenko, H. Chen, S. V. Gratowski, and J. Liang, "Metamaterial-inspired microwave sensor for ethanol detection," in *2022 10th International Symposium on Next-Generation Electronics (ISNE)*, 1–3, Wuxi, China, 2023.